Low-Cost Wide-Angle Beam-Scanning Transmitarray Antennas Using Lens-Loaded Patch Elements: A Proof-of-Concept Study

Wei Hu, Mingyang Dong, Qi Luo, *Senior Member*, *IEEE*, Yuanming Cai, Lehu Wen, Tian-Xi Feng, Wen Jiang, Steven Gao, *Fellow, IEEE*

***Abstract*—In this letter, a novel design concept to achieve a low-cost wide-angle beam-scanning transmitarray (TA) using lens-loaded patch (LLP) elements is presented. In this design, each TA element consists of a beam switchable transmitting element, a group of receiving elements, and a signal via. The received powers of a 2×2 subarray are first combined and then transmitted to the corresponding LLP element, where the phases of the transmitted signals are manipulated for beamforming. Compared to conventional designs, the phase shifters (PSs) can be multiplexed and the number of PSs is effectively eliminated by 75%, which significantly decreases the hardware cost. By employing multiple patches as the feed of the lenses, reconfigurable radiation patterns are obtained, and by properly choosing the transmitting patches, the developed TA achieves a wide-angle 2-D beam-scanning within ±60° with stable gains. To validate the design concept, passive prototypes with a center frequency of 12.5 GHz are simulated, fabricated, and tested. The measured results show that the aperture efficiency is 30.1%, 19.4%, and 14.1% for beams steered to 0°, 30°, and 60° at 12.5GHz, respectively. The beam coverage of ±60° with a less than 3.5-dB scanning loss in the H-plane is obtained.**

***Index Terms*—Low-cost, lens, transmitarray, wide-angle beam scanning.**

I. INTRODUCTION

RECENTLY, wide-angle scanning antenna arrays have received lots of attention due to their wide range of applications, including fifth-generation (5G) wireless communication systems [1]–[4], reconfigurable intelligent surfaces (RISs) [5], [6], and automotive radars [7]. Conventional beam-scanning methods mainly include electronic scanning and mechanical scanning. Electronic scanning antennas, e.g., phased arrays [8], allow very fast beam scanning. However, the cost of the overall antenna system is high. Mechanical scanning antennas, such as a mobile reflector antenna with a multi-axis rotating joint, are bulky in size and have unstable accuracy [9]. The transmitarray (TA) has its own merits of achieving high gain, high flexibility, and low complexity, and it can reduce the consumption and the difficulty in integrating processing [10]–[16]. Therefore, it is a good solution to realize beam steering antennas.

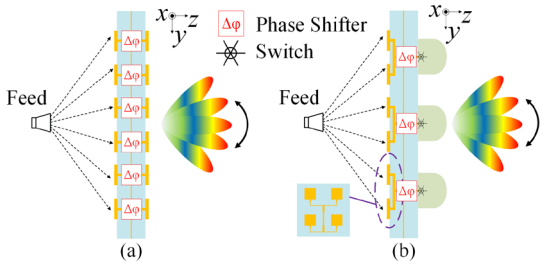

Fig. 1. (a) Traditional beam-scanning TA. (b) Conceptual illustration of the proposed low-cost wide-angle beam-scanning TA.

One method to realize a low-cost beam-scanning TA is through mechanical scanning [17]–[19]. Up to date, most of the reported mechanical beam-scanning TA have a beam coverage of about 80° (±40°). For many applications, the beam coverage is desired to be further extended to cover a larger angle range. Thanks to the well-developed phase array techniques, the use of electronic beam-scanning can increase the beam-scanning range of the TAs. However, similar to the traditional phased arrays, the cost of this solution is high. Although the subarray technique can be applied to eliminate the number of PSs, the beam-steering range of the array is small [20].

The objective of this work is to explore a feasible approach to designing a low-cost wide-angle beam-scanning TA. Inspired by the use of lens array architectures to generate high-gain beams [21][22], a novel concept using the lens-loaded patch (LLP) elements is developed in this study. Fig. 1 shows the concept of the developed TA. As shown, compared to the traditional TA design, instead of connecting one PS to each of the TA elements, the receiving array is divided into subarrays of 2×2 elements and each subarray combines the received power from the feed and then transmits it to the beam reconfigurable LLP element. Therefore, the presented design can eliminate 75% of the PSs compared to a traditional design. Wide-angle beam scanning is theoretically verified at the center frequency of 12.5 GHz. This TA is suitable for 2-D wide-angle

This work was supported in part by the National Natural Science Foundation of China under Grant No. 62071347 and No. 62001348, in part by the Fundamental Research Funds for the Central Universities under Grant XJS210201, in part by EPSRC under Grant EP/N032497/1 and EP/S005625/1, Royal Society IES\R2\212064. *(Corresponding author: Wei Hu.)*.

W. Hu, M. Dong, Y. Cai and W. Jiang are with the National Key Laboratory of Antennas and Microwave Technology, Xidian University, Xi'an 710071, China (e-mail: weihu.xidian@ieee.org).

Qi Luo is with the Department of Engineering and Technology, University of Hertfordshire, AL10 9AB Hatfield, U.K. (e-mail: qiluo@ieee.org).

L. Wen and S. Gao are with the School of Engineering and Digital Arts, University of Kent, CT2 7NT Canterbury, U.K. (e-mail: s.gao@kent.ac.uk).

T.-X Feng is with the Department of Electrical and Computer Engineering, Faculty of Science and Technology, University of Macau, Macau 999078, China (e-mail: feng.tianxi@connect.um.edu.mo).

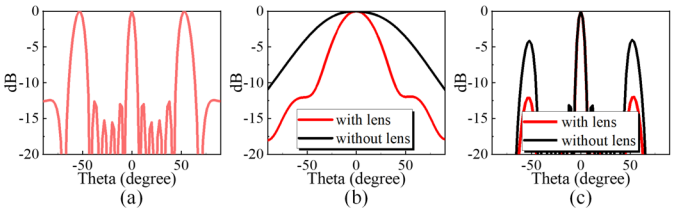

Fig. 2. (a) Array factor, (b) Element factor, (c) Radiation pattern. The array in this calculation consists of 6 × 6 elements and operates at 12.5 GHz, the distance between the element is 1.25 wavelengths.

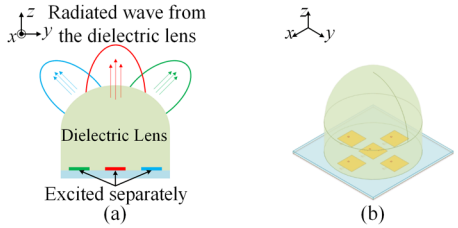

Fig. 3. (a) The ray-tracing of radiated waves from the dielectric lens in a different position. (b) The configuration of a lens is excited by five patches.

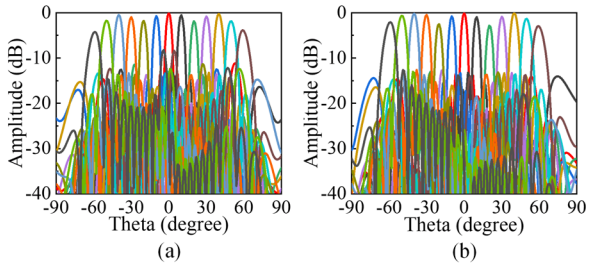

Fig.4. The calculated radiation patterns of the array scanning in (a) xz-plane and (b) yz-plane.

scanning from −60° to 60° through beam sub-regional coverage, and the cost of the TA is significantly reduced by multiplexing PSs. As a proof of concept, passive demonstrators are fabricated and measured.

II. TA Element Design

A. Design Concept

Simply reducing the number of radiating elements in the aperture leads to a sparse array design, which can cause a limited beam-scanning capability. From the array theory [23], the radiation pattern of an array antenna $F(\varphi, \theta)$ can be expressed as:

$$F(\varphi,\theta) = f(\varphi,\theta)\, AF(\varphi,\theta) \tag{1}$$

where $f(\varphi, \theta)$ and $AF(\varphi, \theta)$ are the element factor and array factor, respectively. When the distance between the element is 1.25 wavelengths, the $AF(\varphi, \theta)$ generates grating lobes inevitably. As shown in Fig. 2(a), the position of the grating lobes is about ±54°. In this case, the grating lobes in the $F(\varphi, \theta)$ can be suppressed by changing $f(\varphi, \theta)$. The dielectric lens antenna is known for its high directivity. The element factors of patches with or without lens are shown in Fig. 2(b). The $F(\varphi, \theta)$ calculated by using two different $f(\varphi, \theta)$ are shown in Fig. 2(c). It can be concluded that the grating lobe of $F(\varphi, \theta)$ can be effectively suppressed when $f(\varphi, \theta)$ has high directivity.

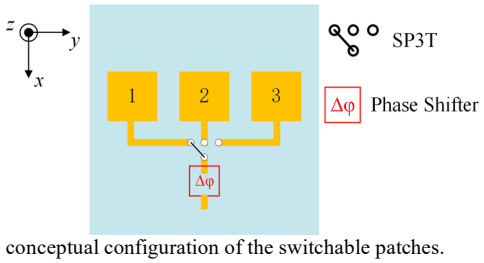

Fig. 5. The conceptual configuration of the switchable patches.

However, this is not enough for wide beam scanning. To improve the beam-scanning range of the array antenna, inspired by [24], if the $f(\varphi, \theta)$ has reconfigurable radiation patterns and the beam can be tilted during the beam-scanning at larger angles, then the total beam-scanning range of the array antenna can be extended. In this design, the beam of the lens can be titled by offsetting the feed of the lens [25], as shown in Fig. 3(a). Thus, it is feasible to obtain reconfigurable and high-directivity beams by using multiple patches to feed the lens. To enable wide-angle 2-D scanning, a configuration of the lens is considered, as shown in Fig. 3(b). To prove this concept, the lens was designed and simulated in ANSYS HFSS. The center frequency is chosen to be 12.5 GHz. The material of the lens is Polytetrafluoroethylene (PTFE) ($\varepsilon_r = 2.9$, $tan\delta = 0.0054$) and the dimensions of the extended hemispherical lens are calculated using the formula given [25]. The simulated radiation pattern of the lens is extracted and then used to calculate the beam-scanning of the array antenna using the $AF(\varphi, \theta)$. The distance between the lenses is chosen to be 30 mm ($1.25\lambda_{12.5GHz}$) and the number of the lenses is 100. Fig. 4(a) and (b) show the calculated radiation patterns of the array scanning in the xz-plane and yz-plane using Fig. 3(b) as the $f(\varphi, \theta)$. During the beam scanning, only one corresponding patch is excited. As shown, the array scans in the wide-angle range of 120° (±60°) with low grating lobes in the xz-plane and yz-plane. It is concluded that the use of five patches as the feeds of the lens is good enough to obtain 2-D wide-angle beam-scanning.

B. Design of The TA Element

To prove the design concept, passive demonstrators were used to validate the beam-scanning performance. As a proof of concept, for the passive demonstrators, instead of using PSs to control the phase of the TA elements, microstrip delay lines of varying lengths are used to mimic the ideal lossless PSs. Considering the available space to route the phase delay lines, instead of using five patches as the feed source of the lens, a linear array of three patches is used. In this configuration, the designed TA performs 1-D beam-scanning.

Fig. 5 shows the design concept of this antenna. Different patches can be excited through the SP3T switch so that the reconfigurable patterns can be obtained. The phase compensation is then performed by PSs to form the phase distribution on the aperture of the array, thus wide-angle beam scanning can be achieved. In addition, the SP3T (MA4SW310) can be selected as the switch with a size of about 1.16 mm × 0.92mm × 0.1 mm with a typical insertion loss of about 0.7 dB at the operating frequency of this design, and the PS (CMD297P34) can be selected which has a size of about 3 mm

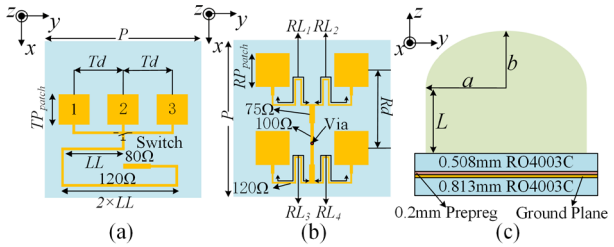

(a) (b) (c)

Fig. 6. The configuration of the proposed TA element. (a) Transmitting patches. (b) Receiving patches (c) Front view. Here, P = 30, TP_{patch} = 5.9, Td=8 (0.33$\lambda_{12.5GHz}$), Rd=15 (0.625$\lambda_{12.5GHz}$), RP_{patch} = 6.2, a = 13, b = 16.3, L = 9.8, (unit: millimeter).

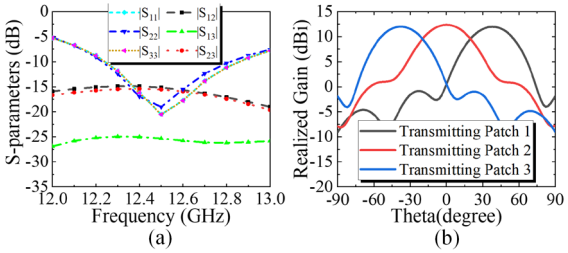

(a) (b)

Fig.7. (a) The simulated amplitude of the S-parameters of LLPs. (b) The radiation pattern in the H-plane when each of the patches is excited at 12.5 GHz.

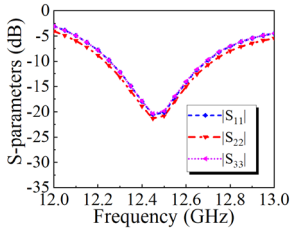

Fig. 8. The circuit simulated amplitude of the S-parameters of LLPs.

× 4 mm × 0.9 mm and a typical insertion loss of 3.2 dB.

In the layout shown in Fig. 6(a), three transmitting patches are printed on a 0.508 mm thick RO4003C substrate (ε_r = 3.55, $tan\delta$ = 0.0027), and an ideal switch is used to control which patch would be excited. When the one patch is connected with the phase delay line, the other two patches are left as open. Fig. 6(b) shows the configuration of receiving subarray, the receiving patches are printed on a 0.813 mm RO4003C substrate. As the feed source radiates spherical waves, the four receiving patches will have a spatial wave path difference. As a result, to maximize the power combing of the receiving subarray, four variable phase delay lines (*RL1*, *RL2, RL3,* and *RL4*) are used for phase compensation. As shown in Fig. 6(c), the position of the lens center is directly above the transmitting patch 2 and the lens is an extended hemispherical lens. Fig 7(a) shows the simulated reflection coefficients of the three patches and their isolation. The EM simulation was performed by considering the periodic boundary conditions. As shown, all patches resonate at 12.5 GHz and the isolation is higher than 14 dB. Fig. 7(b) shows the radiation pattern when each patch is excited. When patch 1 or patch 3 is excited, the beam is titled to ±39° in H-plane (yz-plane) with a realized gain of 12.2 dBi. Since the positions of patches 1 and 3 are relatively symmetrical, their corresponding radiation patterns are also symmetrical. When patch 2 is excited, the patch radiates in the boresight with a realized gain of 12.4 dBi. To assess the

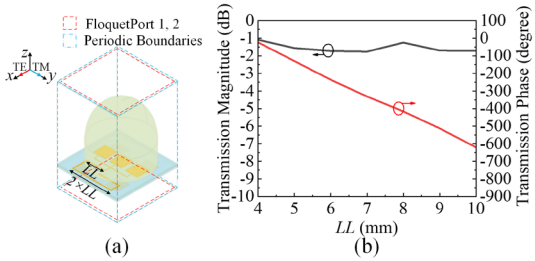

(a) (b)

Fig. 9. (a) The 3D model of the TA element and simulation setup. (b) The simulated transmission coefficients with varied lengths of *LL* at 12.5 GHz.

performance of the proposed beam-switching architecture, three patches with the RF switch circuit [28] were simulated, as shown in Fig. 8. In this figure, $|S_{ii}|$ represents the amplitude of the reflection coefficient when patch i is excited. By comparing the simulation results of the two structures, the switch does not affect the performance of the transmitting patches. Fig. 9(a) shows the 3D model of the developed TA element and the simulation setup. Fig. 9(b) demonstrates the simulated magnitude and phase of the transmission coefficients. When the lengths of the delay line change from 4 mm to 10 mm, a phase change of more than 600° is obtained and the insertion lossless is less than 1.8 dB at 12.5 GHz.

In light of the above discussion, the TA element consists of four patches (2×2 array) on the receiving layer and three LLPs on the transmitting layer. During the beam-scanning in the H-plane, it operates as follows: (1) Scanning in the angle range of −60° to −20°: Patch 3 excited. (2) Scanning in the angle range of −20° to 20°: Patch 2 excited. (3) Scanning in the angle range of 20° to 60°: Patch 1 excited.

III. Design, Simulation, And Measurement of The Transmitarray

Using the developed TA element, a TA consisting of 12×12 receiving patches and 6×6 lens elements was designed. Its aperture size is 180 mm×180 mm×27.6 mm, and the focal height F of the TA is chosen to be 162 mm, corresponding to an F/D ratio of 0.9. The feed is a pyramidal horn with a realized gain of 15.2 dBi at 12.5 GHz. As the concept of the 2×2 subarray is used to receive the incident waves from the feed, after the array size and focal diameter ratio are chosen, the four patches will have a slight difference in spatial phase distributions. Thus, it is necessary to perform some phase compensations for these four patches in order to maximize the power combing efficiency. Fig. 10 shows the spatial phase difference generated by the incident wave on the receiving patches.

To further verify the performance of the beam-scanning TA antenna, thirteen states of TAs with the beams pointing at 0°, ±10°, ±20°, ±30°, ±40°, ±50°, and ±60° in the H-plane are designed and simulated. The simulated far-field beam-scanning radiation patterns in the H-plane of the TA at 12.5 GHz are shown in Fig. 11(a). The peak realized gain is 23.8 dBi at 12.5 GHz in the broadside direction, corresponding to the maximum aperture efficiency of 34.1%. The aperture efficiency is calculated using the formula given in [23]. The peak realized gain is 20.4 dBi while scanning to ±60°. Thus, a beam coverage

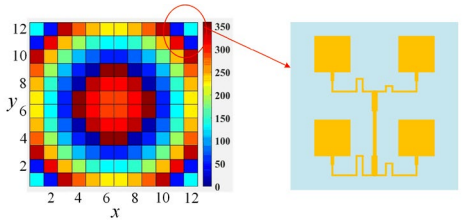

Fig. 10. Calculated spatial phase difference and the phase compensation by microstrip delay line for four patches separately.

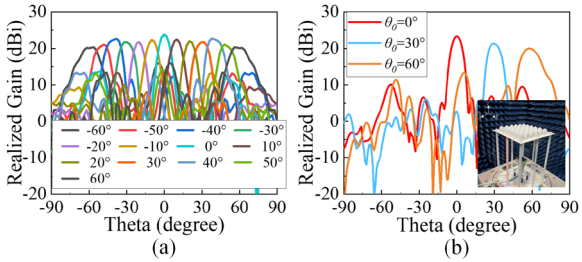

Fig. 11. (a) Simulated radiation patterns in H-plane at 12.5 GHz with different elevation angle θ_0. (b) A photo of the proposed TA under measurement in the anechoic chamber, and measured radiation patterns in H-plane at 12.5 GHz with the elevation angle θ_0 = 0°, 30°, 60°.

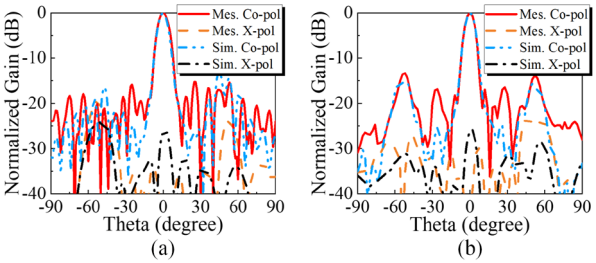

Fig.12. The measured and simulated radiation patterns in the (a) E-plane, (b) H-plane at 12.5 GHz with broadside direction.

of ±60° with a less than 3.5-dB scanning loss is obtained in H-plane. Three prototypes with corresponding beams pointing at broadside and 30° and 60° in the H-plane were fabricated and measured to validate the design concept. Fig. 11(b) shows the developed TA under measurement in the anechoic chamber and the measured radiation patterns with three beam directions. During the beam scanning of the TA, the position of the grating lobes also changes. For example, the maximum grating lobes are about –14 dB (theta = ±54°) at θ_0 = 0°, which corresponds to the transmitting patch 2 in Fig. 7(b). The maximum grating lobes are about –15 dB (theta = –24°) of the beam pointing at θ_0 = 30°, which corresponds to the transmitting patch 1. The maximum grating lobes are about –7 dB (theta = 6°) of the beam pointing at θ_0 = 60°, which also can correspond to the transmitting patch 1. Because of the symmetrical structure of this antenna, the scanning in the other direction is similar to this. Fig. 12 compares the normalized co-polarized and cross-polarized radiation patterns between simulated and measured results in the E-plane and H-plane with broadside direction. Due to the patterns on the E-plane and H-plane of the TA element are not symmetrical, the grating lobes are higher in the H-plane. From the comparison, the grating lobes levels are below −14 dB. The cross-polarization levels are below −25 dB in the E-plane and H-plane.

The measured and simulated gain bandwidth and aperture efficiency in the different beams of the TA are shown in Fig.13. The measured results show that the aperture efficiency is 30.1%, 19.4%, and 14.1% for θ_0 = 0°, 30°, and 60° at 12.5GHz, respectively. The measured 1-dB and 3-dB gain bandwidth are 3.2% (12.2~12.6 GHz) and 7.2% (12~12.9 GHz), respectively. Table I compares the proposed antenna with other reported beam-scanning antennas. The beam-scanning in [17] and [19] is realized by mechanical scanning. Although these methods are low-cost, the beam coverage is small. A wide beam-scanning range of 120° is achieved in [24], yet, this design can only realize 1-D scanning and does not reduce the cost compared to the traditional phased arrays. Compared to these reported designs, the present TA is suitable for 2-D wide-angle beam-scanning at a low cost.

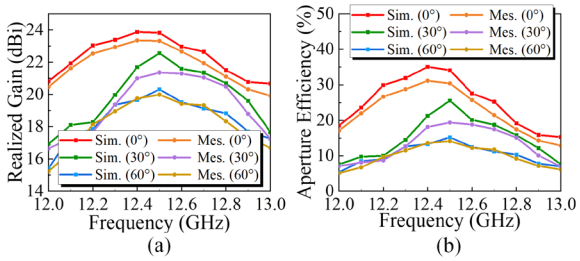

Fig.13. The measured and simulated (a) Gain bandwidth, (b) Aperture efficiency for the different elevation angle θ_0.

TABLE I
COMPARISON OF THE PRESENTED DESIGN WITH OTHERS

Ref.	[14]	[17]	[19]	[24]	[26]	This work
Freq. (GHz)	10	30	70.5	5.8	10	12.5
Max. Beam Coverage	±30° \1-D	±30° \2-D	±43° \1-D	±60° \1-D	±60° \2-D	±60° \2-D
F/D	0.5	0.5	N. A.	N. A.	0.6	0.9
Scanning Loss (dB)	3.13	5	2.7	3	4.15	3.5
Measured Max. Gain (dBi)	25.6	27.8	27	13.2	18.35	23.3
Aperture Efficiency (%)	44.6	29	34	N. A.	34	30.1
Low Cost	No	Yes	Yes	No	No	Yes, reduced no. of PSs

*The gain and aperture efficiency obtained in the Table I do not take into account the losses of phase shifter and switches.

IV. CONCLUSION

In this letter, a novel method is presented to design a low-cost wide-angle beam-scanning TA. This approach realizes low cost by multiplexing PSs, effectively reducing the number of PSs by 75% compared with the traditional beam-scanning TA. It is theoretically proved that the developed TA can realize 2-D wide-angle beam-scanning with an eliminated number of PSs. As a proof of concept, passive prototypes with 1-D beam-steering were designed, simulated, and fabricated. The experimental results show that the developed TA can be steering the beam to wide-angle angles with an eliminated number of PSs.

REFERENCES

[1] S. A. Matos, E. B. Lima, J. S. Silva, J. R. Costa, C. A. Fernandes, N. J. G. Fonseca, and J. R. Mosig, “High gain dual-band beam-steering transmit

array for satcom terminals at Ka-band," *IEEE Trans. Antennas Propag.*, vol. 65, no. 7, pp. 3528–3539, Jul. 2017.

[2] M. H. Dahri, M. H. Jamaluddin, M. I. Abbasi, and M. R. Kamarudin, "A review of wideband reflectarray antennas for 5G communication systems," *IEEE Access*, vol. 5, pp. 17803–17815, 2017.

[3] M. Jiang, Z. N. Chen, Y. Zhang, W. Hong, and X. Xuan, "Metamaterial based thin planar lens antenna for spatial beamforming and multibeam massive MIMO," *IEEE Trans. Antennas Propag*., vol. 65, no. 2, pp. 464–472, Feb. 2017.

[4] Y. Hu, W. Hong, and Z. H. Jiang, "A multibeam folded reflectarray antenna with wide coverage and integrated primary sources for millimeter-wave massive MIMO applications," *IEEE Trans. Antennas Propag*., vol. 66, no. 12, pp. 6875–6882, Dec. 2018.

[5] L. Dai, B. Wang, M. Wang, X. Yang, J. Tan, S. Bi, S. Xu, F. Yang, Z. Chen, M. D. Renzo, C. B. Chae, and L. Hanzo, "Reconfigurable intelligent surface-based wireless communications: Antenna design, prototyping, and experimental results," *IEEE Access*, vol. 8, pp. 45913–45923, 2020.

[6] J. Wang, Y. -C. Liang, J. Joung, X. Yuan, and X. Wang, "Joint beamforming and reconfigurable intelligent surface design for two-way relay networks," *IEEE Trans. Commun.*, vol. 69, no. 8, pp. 5620–5633, Aug. 2021.

[7] S. B. Yeap, X. Qing, and Z. N. Chen, "77-GHz dual-layer transmitarray for automotive radar applications," *IEEE Trans. Antennas Propag*., vol. 63, no. 6, pp. 2833–2837, Jun. 2015.

[8] S. Ye, X. Liang, W. Z. Wang, R. H. Jin et al., "High-gain planar antenna arrays for mobile satellite communications," *IEEE Antennas Propag. Mag.*, vol. 54, no. 6, pp. 256–268, Dec. 2012.

[9] Y.-L. Yao, F.-S. Zhang, and F. Zhang, "A new approach to design circularly polarized beam–steering antenna arrays without phase shift circuits," *IEEE Trans. Antennas Propag*., vol. 66, no. 5, pp. 2354–2364, May 2018.

[10] K.-W. Lam, S.-W. Kwok, Y. Hwang, and T. K. Lo, "Implementation of transmitarray antenna concept by using aperture-coupled microstrip patches," in *Proc. Asia-Pacific Microw.*, 1997, pp. 433–436.

[11] Q. Luo, S. Gao, M. Sobhy, and X. Yang, "Wideband transmitarray with reduced profile," *IEEE Antennas Wireless Propag. Lett*., vol. 17, no. 3, pp. 450–453, Mar. 2018.

[12] Q. Luo, S. Gao, M. Sobhy, X. Yang, Z.-Q. Cheng, Y.-L. Geng, and J. T. S. Sumantyo, "A hybrid design method for thin panel transmitarray antennas," *IEEE Trans. Antennas Propag.*, vol. 67, no. 10, pp. 6473–6483, Oct. 2019.

[13] F. F. Manzillo, A. Clemente, and J. L. González-Jiménez, "High-gain D-band transmitarrays in standard PCB technology for beyond-5G communications," *IEEE Trans. Antennas Propag*., vol. 68, no. 1, pp. 587–592, Jan. 2020.

[14] P.-Y. Feng, S.-W. Qu, and S. Yang, "Phased transmitarray antennas for 1-D beam-scanning," *IEEE Antennas Wireless Propag. Lett.*, vol. 18, no. 2, pp. 358–362, Feb. 2019.

[15] W. Hu, J. S. Dong, Q. Luo, Y. M. Cai, X. K. Liu, L. H. Wen, W. Jiang, and S. Gao, "A wideband metal-only transmitarray with two-layer configuration," *IEEE Antennas Wireless Propag. Lett.*, vol. 20, no. 7, pp. 1347–1351, Jul. 2021.

[16] M. Sazegar, Y. L. Zheng, C. Kohler, H. Maune, et al., "Beam steering transmitarray using tunable frequency selective surface with integrated ferroelectric varactors," *IEEE Trans. Antennas Propag.*, vol. 60, no. 12, pp. 5690–5699, Dec. 2012.

[17] N. Gagnon and A. Petosa, "Using rotatable planar phase shifting surfaces to steer a high–gain beam," *IEEE Trans. Antennas Propag*., vol. 61, no. 6, pp. 3086–3092, Jun. 2013.

[18] M. U. Afzal and K. P. Esselle, "Steering the beam of medium to high gain antennas using near–field phase transformation," *IEEE Trans. Antennas Propag*., vol. 65, no. 4, pp. 1680–1690, Apr. 2017.

[19] L. -Z. Song, P. -Y. Qin, S. -L. Chen, and Y. J. Guo, "An elliptical cylindrical shaped transmitarray for wide-angle multibeam applications," *IEEE Trans. Antennas Propag,* vol. 69, no. 10, pp. 7023–7028, Oct. 2021.

[20] R. J. Mailloux, Phased Array Antenna Handbook, Artech House, Inc., 2005.

[21] M. Arias Campo, D. Blanco, S. Bruni, A. Neto, and N. Llombart, "On the Use of Fly's Eye Lenses with Leaky-Wave Feeds for Wideband Communications," *IEEE Trans. Antennas Propag*., vol. 68, no. 4, pp. 2480-2493, Apr. 2020.

[22] S. Bosma, N. van Rooijen, M. Alonso-delPino, and N. Llombart, "High Aperture Efficiency Plastic Lens Antenna for Scanning Lens Phased Array at 180 GHz," *2021 46th International Conference on Infrared, Millimeter and Terahertz Waves (IRMMW-THz),* Chengdu, China, 2021, pp. 1-2.

[23] C. A. Balanis, *Antenna Theory Analysis and Design*, 3rd ed. Hoboken, NJ, USA: Wiley, 2005.

[24] Y. Bai, S. Xiao, M. Tang, Z. Ding, and B. Wang, "Wide-angle scanning phased array with pattern reconfigurable elements," *IEEE Trans. Antennas Propag*., vol. 59, no. 11, pp. 4071–4076, Nov. 2011.

[25] X. Wu, G. V. Eleftheriades, and T. E. van Deventer-Perkins, "Design and characterization of single- and multiple-beam mm-wave circularly polarized substrate lens antennas for wireless communications," *IEEE Trans. Microw. Theory Techn.*, vol. 49, no. 3, pp. 431–441, Mar. 2001.

[26] Z. F, Y. G-M, J. Y-Q. Low-Profile Circularly polarized transmitarray for wide-angle beam control with a Third-Order Meta-FSS [J]. *IEEE Trans. Antennas Propag*., vol. 68, no. 5, pp. 3586–3597, May. 2020.

[27] J. R. James, P. S. Hall, and C. Wood, *Microstrip Antenna Theory and Design*, Stevenage England: Peter Peregrinus, 1981.

[28] MACOM. MA4SW310 HMIC SP3T Silicon PIN Diode Switch. [Online]. Available: https://cdn.macom.com/datasheets/MA4SW310.pdf